
埋め込み型人工心臓器使用時の感染防御に有用な駆動ライン被覆材および新規皮膚貫通部被覆デバイスの開発

水野敏秀, 巽 英介, 妙中義之

循環器病研究の進歩(通巻48号)
Vol.XXIX No.1(2008.11)p.71~78

埋め込み型人工心臓器使用時の感染防御に有用な駆動ライン被覆材および新規皮膚貫通部被覆デバイスの開発

水野敏秀*, 巽 英介*, 妙中義之*²

はじめに

日本国内における心臓移植の開始とともに、人工心臓は重症心不全患者の移植までのブリッジ使用を目的とする重要な治療手段の1つとして改めて認識されている。国内で心臓移植を受けた患者65例の75%は、移植に至るまでの間、補助人工心臓により全身循環を維持されていた症例である(2007年9月まで)¹⁾。そのため全世界的に重症心不全患者に対する人工心臓の有用性は再認識され、海外と同様に、より快適な人工心臓システムの開発が急務となっている。

現在、国内では補助人工心臓は血液ポンプ

および駆動装置を体外に設置し、コンデュ部を経て体内臓器に連続している形式が主に使用されている。また、近年血液ポンプおよび駆動部を体内に設置する補助人工心臓の使用が増加し、より長期の施行や在宅での治療が可能となっている。しかしながら、埋め込み型の人工心臓においても駆動ラインやベントチューブなど体内と体外を連続する機器が依然として存在し、かかる体内・体外を連続する部位の存在は、外界より侵入する病原体の感染門戸として開発当初より問題視されている²⁾。そして、心不全患者に対する心臓移植までの人工心臓による循環補助を行う本治療手段において、“感染による合併症”はその成績を左右する悪因子の1つである³⁾。

また、人工心臓の開発や人工心臓療法での臨床技術が向上したことにより、人工心臓を装着する期間が長期におよぶ症例が多くなっており、本治療期間の長期化が感染症併発を高確率にし、重篤な症状を呈する症例が指摘されている⁴⁾。事実、海外の報告からもICD-9で分類された1999~2005年までの補助人工心臓装着者について、その疾病報告により、60症例中の72%に人工心臓装置に関連する感染症の発生を認め、そのうち29例はDriveline infectionが原因であったことが報告されている。かかる感染症発症率は、補助の長期化に従い高くなることが明らかで、感染症を併発していた患者には、移植後に心内膜炎を発症することが多く、同じ原因菌による感染が認められることが指摘されている⁵⁾。したがって、移植へのブリッジにおいて“感

Key word

ventricular assist system
driveline infection
skin penetrating pad
segmented polyurethane
porous material

Development of a novel skin penetrating pad for driveline infection in the long-term therapy with implantable ventricular assist system

*Toshihide Mizuno, Eisuke Tatsumi :

Department of Artificial Organs,
Advanced Medical Engineering center,
National Cardiovascular Center Research Institute
国立循環器病センター研究所
先進医工学センター 人工臓器部

²Yoshiyuki Taenaka :

Deputy Director,
National Cardiovascular Center Research Institute
国立循環器病センター研究所 副所長

染による合併症”の発生は、その予後を決定する重要な因子であり、その重要な感染門戸として皮膚を貫通し体内と体外を連続する機器の存在は、現在においても十分に検討されるべき問題点である。

Driveline infectionは、皮膚刺入部周囲の表皮組織が駆動ラインに沿って体内に陥入し(表皮のダウングロース、形成される死腔を主な感染源とし、この死腔内における細菌繁殖や出血が、人工心臓の長期施行時におけるDriveline infectionを増悪させる要因の1つと考えられている(図1)。現在、Driveline infectionを防止するためには、皮膚貫通部への抗生物質の定期的な塗布が効果的であるとされているが⁷⁾、治療期間の長期化に伴い、新たな薬剤耐性菌への対策など、課題がいまだ多く残っている。

本研究では、人工心臓のDriveline infectionを防止することを目的とし、駆動ライン表面と周囲の生体組織を強固に接着させることが可能で、柔軟かつ生体適合性に優れ、長期的な生体内留置が可能なセグメント化ポリウレタン製多孔体を開発し⁸⁾、実際の使用時に駆動ライン表面と周囲組織を癒着させるために最適な多孔体素材の物性、孔径および生体組織の浸潤性について検討を行った。さらに本多孔体素材を独特な形状に加工することにより、駆動ライン皮膚貫通部における表皮のダウングロースを防止し、駆動ラインへの外力による周囲組織との傷害を抑制可能な新規皮膚貫通パッドを考案し、それを人工心臓用駆動ラインに応用するために形状や素材について最適化を行った。

本研究で行われた動物実験は、国立循環器

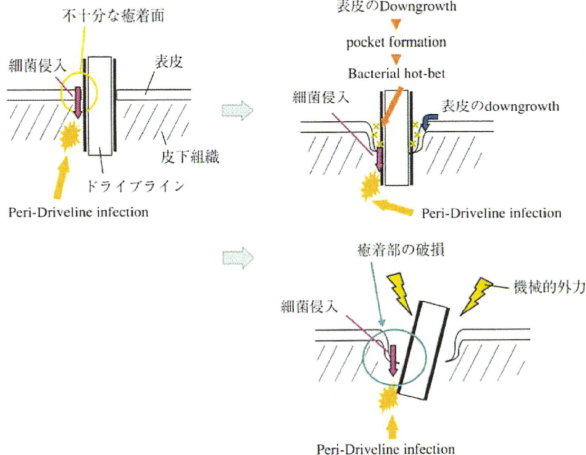


図1. Driveline infectionの発生機序

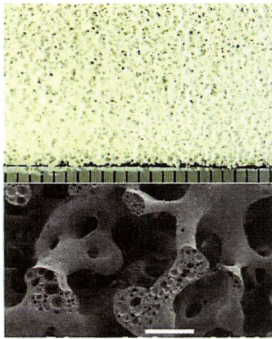
病センター動物実験委員会の承認のもと、同動物実験指針に基づき行われた。

1. セグメント化ポリウレタン製新規多孔体の開発

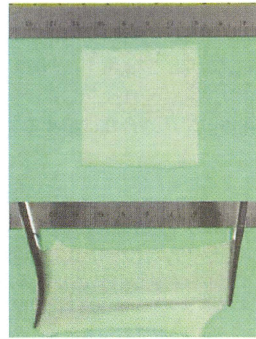
我々が新規に開発したセグメント化ポリウレタン多孔体は、その孔径を約50～500 μ mの範囲で自由に調節し、比較的太い骨格から構成される三次元網状構造体で、その骨格内も約10～50 μ m径の微小孔を多数有する構造体である(図2)。本多孔体は、新製法により表層に緻密層が生成せず、スライス処理による緻密層除去が不要のため曲面を有するさまざまな形状に形成することが可能である。

本実験では、種々の孔径の多孔体を作製し、孔径の変化と物性について検討を加えた。本素材の孔径および孔径分布の測定については、走査電子顕微鏡(SM200, TOPCON TECHNOHOUSE CORPORATION, Tokyo,

Japan)およびマイクロSCOPE(VH-6300, キーエンス, Osaka, Japan)にて撮影を行い、撮影画像の同一表面上の孔部分を手作業で抽出し、再度コンピュータ上に取り込んだ上で、画像処理システム(LUZEX AP, ニレコ社, Tokyo, Japan)にて孔径および孔径分布を測定した。引張試験は平均孔径約500, 300および50 μ mの新規開発多孔体を作製し(n=3), 精密万能試験機(オートグラフAG-1, SHIMAZU, Kyoto, Japan)を使用し、ロードセル50N, ダンベル形状DIM3号, 引張速度100mm/min, 標線間距離10mm, チャック間距離30mmで行った。引張強度試験については、引張圧縮試験機(インテスコ205B, INTESCO, Chiba, Japan)を用い、チャック間距離10mm, 引張速度50mm/minによって定法により測定した。多孔体は平均孔径約300 μ mのものを使用し(n=5), 破断強度(N/cm²)と破断時の伸展率を測定した。



3-D reticulated microstructure
(diameter of pore : 50 ~ 500 μ m)



Sufficient mechanical strength and flexibility

図2. 新規開発されたセグメント化ポリウレタン製多孔体

新規多孔体は、組織刺激性の少ない熱可塑性ウレタンからなる三次元網状構造の多孔体で、本素材は適切な強度と柔軟性を保持し、さまざまな形状に加工することが可能で、耐久性にも優れている。

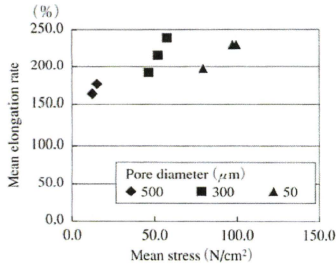


図3. 新規多孔体の引張強度試験結果

その結果、新規多孔体の物性として、引張試験で平均孔径500 μm の多孔体は、平均応力13.1N/cm²で平均進展率167%、平均孔径300 μm の多孔体で平均応力52.3N/cm²で平均進展率215%、平均孔径50 μm の多孔体は平均応力92.0N/cm²で平均進展率219%を示し(図3)、引張強度試験で破断強度は、平均孔径300 μm の多孔体において、30.6 \pm 1.5N/cm²であり、破断時の進展率は46.1 \pm 10.1%であった。

II. 新規多孔体の生体適合性に関する研究

本実験では、本多孔体素材の孔径の違いに伴う組織浸潤性の変化を検討するために、円柱状に成形した平均孔径約500、450、300、250、150、100および50 μm の多孔体を両端が開口したシリコンチューブ内(内径3mm)に挿入した試料を作製した。体重60kgの雌ヤギを1頭用い、イソフルランによる全身麻酔下背部の皮下組織内に各孔径の試料を外科的に埋め込んだ(n=5)。4週間後、ヤギを安楽死させ、埋め込んだ試料を周辺組織ごと摘出し、10%中性緩衝ホルマリン溶液で固定した。摘出した試料は、その長軸に沿って

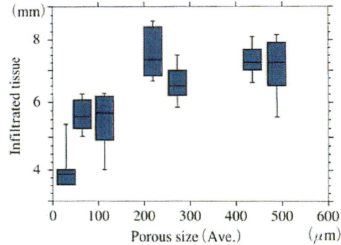


図4. 新規多孔体内への組織浸潤試験結果

切り出し、薄層切片を作製、Azan染色を行った後に光学顕微鏡による観察を行った。開口していた端部より、チューブ内に侵入した肉芽組織の量およびその病理組織像について検討を行った。

1カ月の生体への埋入後、摘出された新規多孔体への組織浸潤性の検討用試験チューブの組織学検討では、円柱状の多孔体両端より肉芽組織が浸潤し、多孔体と生体由来の組織の分離は非常に困難であった。試験チューブ内の平均孔径50、150、300および500 μm の多孔体について、それぞれの肉芽組織浸潤長は4.0 \pm 0.7、5.4 \pm 0.9、6.6 \pm 0.6および7.2 \pm 1.2cm(n=5)であり、孔径が50~300 μm にかけては孔径が大きくなるにつれて組織浸潤長は大きくなる傾向が見られた。孔径300 μm 以上では組織浸潤長は約7.0mmでプラトーとなった(図4)。病理組織学的には特に孔径の大きいグループの多孔体(孔径300および500 μm)では、膠原線維を主体とする成熟した結合組織浸潤が良好であった(図5)。

III. 新規多孔体素材を用いた人工心臓駆動ライン用カフおよび皮膚貫通パッドの開発

我々の新規皮膚貫通パッドは、本多孔体素

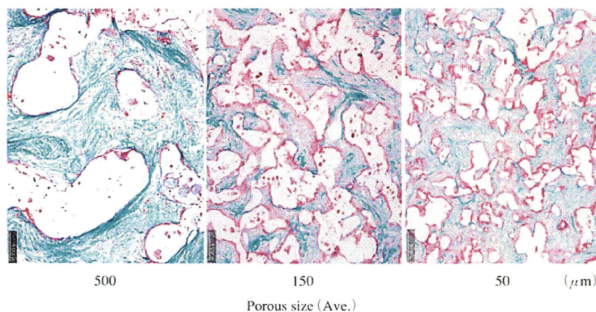


図5. 新規多孔体内へ浸潤した肉芽組織

特に孔径の大きいグループ(孔径500および300 μm)ほど、組織学的に多孔体内には膠原線維を主体とする成熟した結合組織浸潤が良好であり、同部には新生した血管組織も頻繁に観察された。また、感染、壊死などの所見は認められなかった。

材を使用した類円状の三層フランジ形状を有し、人工心臓駆動ラインの皮膚貫通部に外科的に設置されるものである(図6)。このフランジ部の最下層は組織浸潤性を重視した大孔径の多孔体で、表皮への血流を阻害することなく皮下組織と一体化する。また、やや小孔径の多孔体で作られる中間層は、表皮との接着およびダウングロース抑制の役割を担う。さらに無孔質パッドからなる最上層は、汚染されやすい駆動ラインをフランジ外縁の皮膚接合部から隔離するとともに、駆動ラインへの外力を吸収し、創部を保護することを目的としている。この構造により、本デバイスでは皮膚貫通部において極めて強固な皮膚との癒着が得られ、同時に高い抗感染性ももたらされると考えられる(図7)。本新規開発品の生体適合性および出口部感染症の防止効果を検討するため、本皮膚貫通パッド部のみの試作品を作製し、成ヤギの背部皮膚に外科的に装着し、約2年間の装着実験を行った。術後において、本装着部は術後の急性期を除き、消

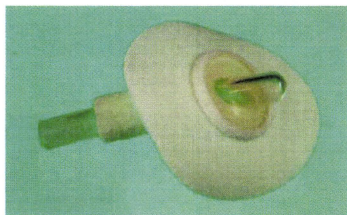


図6. 人工心臓駆動ライン用皮膚貫通パッド

皮膚貫通パッドは、新規開発された多孔体を用いた体内のドライラインを被覆すると同時に皮膚貫通部に三層からなる類円状のフランジ部を設けたもので、極めて単純な構造および材料から構成されている。

毒・ドレーピングなどは全く行わなかった。

本皮膚貫通デバイスは、最長2年間の経過中にデバイス周囲の皮膚の発赤、腫脹や排膿などの感染徴候や異物排除の反応により自然に脱落するような徴候は全く認められず、皮膚と強固に接着していた。毎日、駆動ライン

部分を多方向へ強く牽引したが、皮下でのフレンジの動揺や皮膚貫通パッドの損傷は全く見られなかった(図8)。摘出した標本を皮下組織側から観察したところ、フレンジ部分は豊富な血管新生を伴う組織で覆われていた。

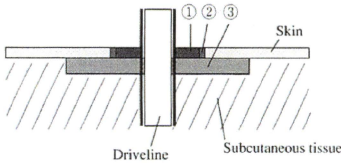


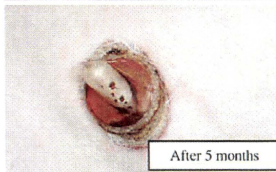
図7. 皮膚貫通パッドの横断面図

- ①無孔質パッドで作成され、汚染されやすい駆動ラインをフレンジ外縁の皮膚接合部から隔離するとともに、駆動ラインへの外力を吸収し、創部を保護する。
- ②表皮との接着およびダウングロス抑制の役割を担う。
- ③組織浸潤性を重視し、表皮への血流を阻害することなく皮下組織と一体化する。

<Results>

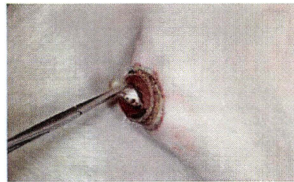


After 1 day



After 5 months

No wound care (disinfection and draping) except for acute phase immediately after surgery



Pad was strongly pulled

図8. 長期動物実験による皮膚貫通パッドの生体適合性試験結果

皮下の膿瘍形成なども認めなかった。次に、駆動ラインに沿う方向で標本を切開し観察したが、最上層の外縁で表皮のダウングロスに伴う死腔形成は認めなかった。最下層の多孔体は豊富な組織浸潤により周囲組織と一体化しており、剥離することはできなかった(図9)。また、摘出後ドライラインの被覆カフ部の組織学的検討では、ポリエステル製のカフと比較し、線維間に侵入した肉芽組織は、線維芽細胞を主体とする細胞成分が豊富な幼弱な肉芽組織が主体であったが、本多孔体製のカフ内に浸潤した肉芽組織はコラーゲン線維を主体とする成熟した組織であることが観察された(図10)。

まとめ

本実験で、新規に開発された多孔体素材は、生体内埋め込み材料として周囲組織との強固な癒着を実現する材料として使用され、十分な肉芽組織が浸潤可能な孔径を有しながら、周囲の生体組織に負担の少ない柔軟性と外力

に対する強度を持ち、長期留置可能な素材であることが示された。また、本多孔体に浸潤した肉芽組織は、本実験で使用したポリエステル製の不織布と比較して、コラーゲン線維が豊富で、成熟した形態であり、長期の癒着を維持することに有用であることが示された。さらに、本実験で使用された新規皮膚貫通パッドは、約2年間にわたる装着時において、消毒などの創部管理を行わなかったにもかかわらず、感染や周囲組織の壊死など Driveline infection の所見は認められず、表皮のダウングロースの抑制に効果的であることが示された。

現在では、人工心臓本体の開発の進展や術後管理手法の向上に伴い長期的に安定した治療を行うことが可能になっている。しかしながら、認知症患者や小児患者など、治療に対する理解の乏しい患者への長期的な施行に関しては、創部の清潔な保持や、外力からの駆動ラインの保護を十分に行うことが困難であ

ると思われる。かかる問題において、我々の開発した皮膚貫通パッドおよびカフ付き駆動ラインは、駆動ラインに対する外力に対し非常に強い皮膚との癒着性を示し、日常的な創部管理を最小限の労力で行うことが可能であると考えられ、長期化する人工心臓療法を、より安全に行うための装置として本治療法の普及に貢献できるものと考えられた。

結 論

新規開発のセグメント化ポリウレタン多孔体は、強度、柔軟性、耐久性、組織親和性および組織浸潤性に優れている。この多孔体を用いて作製した皮膚貫通パッドと生体組織との結合は強固で、駆動ラインの皮膚貫通部でダウングロースを引き起こさないため、出口部感染の防止に有用であると考えられる。

§ 文 献

- 1) 中谷武嗣, 北村慧一郎: 日本臨床補助人工心臓研究会, 2007年度補助人工心臓レジストリー, 人

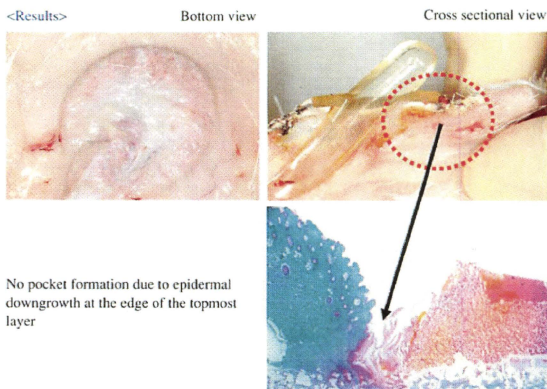


図9. 皮膚貫通パッド装着6カ月後の摘出像およびその組織学的観察

<Results> Histological tests of the covering materials at 6 months-animal implantation
Polyester vs. SPU porous material

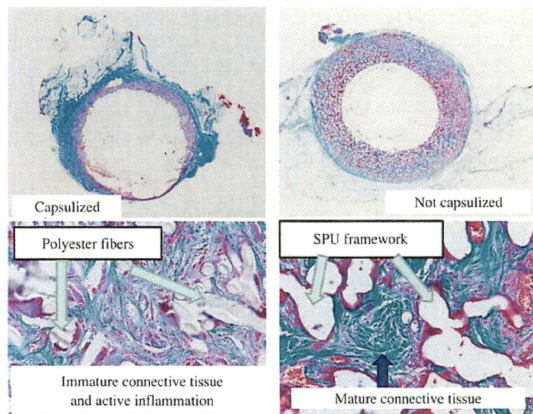


図10. ドライライン被覆カフ部の病理組織像
 ポリエステル製のカフと比較し、新規多孔体による被覆カフ (SPU) は、周囲組織のカプセル化を抑制している。また、多孔体内に浸潤した膠原線維は成熟した形態を示し、前者と比較し、強固な癒着を形成している。

工臓器 2008;37(1):8-13.
 2) Tatsumi E, Nakatani T, Imachi K, et al : Domestic and foreign trends in the prevalence of heart failure and the necessity of next-generation artificial hearts : a survey by the Working Group on Establishment of Assessment Guidelines for Next-Generation Artificial Heart Systems. J Artif Organs 2007;10(4): 187-94.
 3) Kanter KR, McBride LR, Pennington DG, et al : Bridging to cardiac transplantation with pulsatile ventricular assist devices. Ann Thorac Surg 1988; 46(2):134-40.
 4) Zierer A, Melby SJ, Voeller RK, et al : Late-onset driveline infections: the Achilles' heel of prolonged left ventricular assist device support. Ann Thorac Surg 2007;84(2):520-1.

5) Griffith BP, Kormos RL, Nastala CJ, et al : Results of extended bridge to transplantation : window into the future of permanent ventricular assist devices. Ann Thorac Surg 1996;61(1):396-8.
 6) Monkowski DH, Axelrod P, Fekete T, et al : Infections associated with ventricular assist devices : epidemiology and effect on prognosis after transplantation. Transpl Infect Dis 2007;9(2):114-20.
 7) Choi L, Choudhri AF, Pillarisetty VG, et al : Development of an infection-resistant LVAD driveline : a novel approach to the prevention of device-related infections. J Heart Lung Transplant 1999;18(11): 1103-10.
 8) 岡本吉弘, 根本泰, 黄海瑛, 他 : 組織工学用三次元ポリウレタン多孔質スキャホールド材の開発. 人工臓器 2005;34(2):S-100.

Thoughts and Progress

An Animal Study of a Newly Developed Skin-Penetrating Pad and Covering Material for Catheters to Prevent Exit-Site Infection in Continuous Ambulatory Peritoneal Dialysis

*†Masato Aoyama, †Toshihide Mizuno,
†Eisuke Tatsumi, †Yoshiyuki Taenaka,
‡Yasushi Nemoto, ‡Yoshihiro Okamoto,
*Yoshiaki Takemoto, *Toshihide Naganuma,
and *Tatsuya Nakatani

*Department of Urology, Osaka City University Medical School, Osaka; †Department of Artificial Organs, Research Institute, National Cardiovascular Center, Suita; and ‡Development Department, Chemical Products Division, Bridgestone Corporation, Yokohama, Kanagawa, Japan

Abstract: Because currently available peritoneal dialysis catheters are not sufficiently biocompatible with the skin and subcutaneous tissue at the site of penetration, exit-site infection due to pericatheter pocket formation caused by epidermal downgrowth over a long period of time has increasingly become a problem. We developed a new, biocompatible, segmented polyurethane porous material and devised a novel skin-penetrating pad, the form and material of which we optimized for application in peritoneal dialysis catheters. For the extent of tissue ingrowth into this porous material to be examined, test materials with different pore diameters were inserted into hollow silicone tubes and implanted in the subcutaneous tissue of a goat. Four weeks later, the tubes were extracted, and, after the extent of granulation tissue ingrowth was measured, histopathological evaluation was made. Our novel skin-penetrating pad has three disklike layers of the segmented polyurethane material with different pore sizes, into the center of which a polyurethane catheter is inserted. These pads were implanted in the skin of a goat and clinically observed over a 2-year period, after which they were extracted and histopathologically analyzed. In accordance with actual clinical procedures, a commercial CAPD catheter equipped with our skin-penetrating pad was left indwelling in a goat for 4 months, and the performance of the pad was evaluated after repeated periodic infusion and drainage of

the dialysate in and out of the abdominal cavity. There was no inflammation of the ingrown tissue in the pores of the segmented polyurethane material as well as the surrounding tissue, which indicated favorable tissue biocompatibility. The extent of tissue ingrowth was greater as the pore size of the material was larger, and the tissue tended to be mature, mainly consisting of collagenous fibers. The skin-penetrating pad using the porous material, of which tissue ingrowth was thus optimized, tightly adhered to the goat skin throughout the 2-year experimental period without any special wound care such as cleansing or disinfection. The performance of the skin-penetrating pad was similarly favorable when attached to a commercial continuous ambulatory peritoneal dialysis catheter. The newly developed segmented polyurethane porous material had excellent tissue biocompatibility and tissue ingrowth. The skin-penetrating pad devised by using this porous material did not cause epidermal downgrowth, suggesting that it may be effective for the prevention of exit-site infection. **Key Words:** Skin-penetrating pad—Continuous ambulatory peritoneal dialysis—Exit-site infection.

In continuous ambulatory peritoneal dialysis (CAPD), which is an effective therapeutic procedure for chronic renal failure and end-stage renal disease, the prevention of catheter exit-site infection is one of the most important challenges in conducting long-term treatment safely (1). The main source of this infection is the dead space that is formed by epidermal invagination along the catheter (epidermal downgrowth) at the site of skin penetration (2), and bacterial proliferation and bleeding in these pockets are considered to exacerbate infection during CAPD (3). For this exit-site infection to be prevented, the periodic topical application of antibiotics on the skin is considered effective, but, despite increasing treatment periods, measures against drug-resistant bacteria have yet to be established (4,5). Moreover, for the CAPD catheter to be firmly attached to the surrounding living tissue, devices such as an alumina ceramic percutaneous terminal, titanium fiber mesh skin-penetrating device, expanded polytetrafluoroethylene skin-penetrating device, and solid polyurethane catheter covering material have been developed, and attempts have been made to apply them to catheters, but none have been put to practical use (6–9).

In this study, in order to prevent exit-site infection, we developed a segmented polyurethane porous material that is flexible and biocompatible and can be subjected to long-term indwelling, and

doi:10.1111/j.1525-1594.2009.00805.x

Received March 2008; revised October 2008.

Address correspondence and reprint requests to Dr. Masato Aoyama, Department of Urology, Osaka City University Medical School, 4-3 Asahimachi 1-chome, Abeno-ku, Osaka, 545-8585, Japan. E-mail: masatoaym@msic.med.osaka-cu.ac.jp

investigated its optimal properties, pore size, and tissue ingrowth so that the catheter can tightly adhere to the surrounding tissue during actual use. Furthermore, we created a novel skin-penetrating pad by devising a unique form to prevent epidermal downgrowth and to inhibit damage of the surrounding tissue by external pressure to the catheter and optimized its form and material for application in CAPD catheters.

MATERIALS AND METHODS

Development of a new, segmented polyurethane porous material

We newly developed a segmented polyurethane porous material using Mirastran (E980, Nippon Mirastran, Kanagawa, Japan), a polycarbonate segmented polyurethane resin. This material, whose pore diameter can be freely adjusted within the range of approximately 100–1000 μm , had a three-dimensional reticulated microstructure consisting of a relatively thick framework, with many micropores of approximately 10–50 μm in pore diameter within the framework (Fig. 1). This porous material does not produce a dense surface layer due to a new manufacturing process and can be formed into various shapes with a curved surface, as the removal of dense layers by slicing is not necessary (Fig. 2). In this study, we prepared test materials with different pore sizes and evaluated the changes in their properties. For the measurement of pore size and its distribution, images were taken and examined by using a scanning electron microscope (SM200, Topcon Technohouse Corporation, Tokyo, Japan)

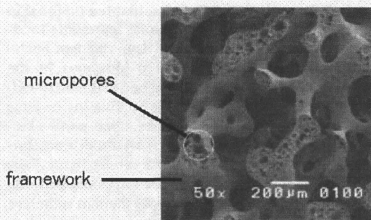


FIG. 1. Scanning electronmicrograph photograph of the new porous material. The segmented polyurethane porous material has a three-dimensional reticulated microstructure consisting of a relatively thick framework with many micropores of approximately 10–50 μm in pore diameter within the framework.

Artif Organs, Vol. 33, No. 12, 2009

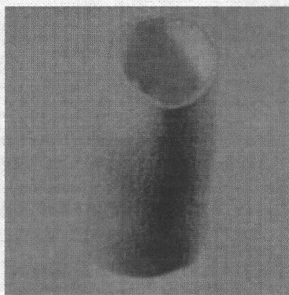


FIG. 2. Photograph of the lube-shaped porous material. Our material can be formed into complicated shapes while maintaining its continuous porous microstructure.

and a microscope (VH-6300, Keyence Corporation, Osaka, Japan). The pores on the same surface of the images were manually extracted and uploaded again onto our computer, and the pore size and its distribution were measured by using an image processing system (LUZEX AP, Nireco Corporation, Tokyo, Japan). Test materials with mean pore diameters of 490, 290, and 41 μm were prepared ($n = 3$), and the tensile testing was conducted at load cell of 50 N, dumbbell-shape DIM 3 type, tensile rate of 100 mm/min, gauge length of 10 mm, and chuck distance of 30 mm by using a precision universal tensile testing machine (Autograph AG-1, Shimadzu, Kyoto, Japan).

Biocompatibility of the newly developed porous material

For the changes in the extent of tissue ingrowth according to the pore size of this material to be studied, cylindrically shaped test materials with pore diameters of 500, 300, 150, and 50 μm inserted in open-ended silicone tubes (length: 3 cm, inner diameter: 3 mm, $n = 5$) were prepared (Fig. 3). These test materials were surgically implanted in the subcutaneous tissue on the back of an adult female goat weighing 60 kg under general anesthesia with isoflurane. Four weeks later, the goat was euthanized, and the test materials were extracted along with the surrounding tissue and fixed in 10% neutral buffered formalin. The extracted materials were sliced longitudinally to prepare thin sections, which were examined by using a light microscope after Azan staining. The extent of granulation tissue ingrowth in the tube

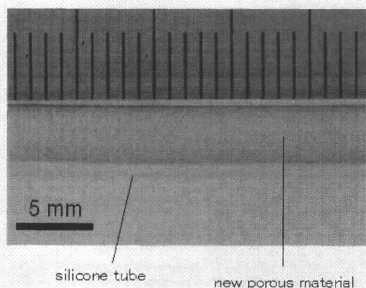


FIG. 3. Photograph of the test material.

from the open end was measured, and its histopathological findings were investigated.

Development of a novel CAPD catheter skin-penetrating pad and cuff using the newly developed porous material

Our novel skin-penetrating pad has three disklike layers of the segmented polyurethane material, which is surgically implanted at the site of catheter penetration. The lowest flange-shaped layer of this pad consisting of large pore size material due to its favorable tissue ingrowth was designed to adhere to the subcutaneous tissue without inhibiting blood flow to the epidermis. The middle layer consisting of slightly smaller pore size material was intended to adhere to the epidermis and prevent downgrowth. The topmost layer made of nonporous material was designed to separate the catheter, which is subject to contamination, from the outer edge of the flange part that adheres to the skin as well as protect the wound

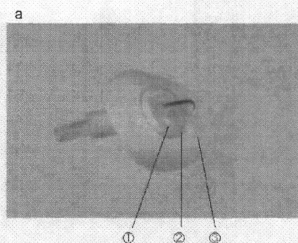


FIG. 4. (a) Photograph of the new skin-penetrating pad. (b) Illustration of the new skin-penetrating pad implanted in the skin.

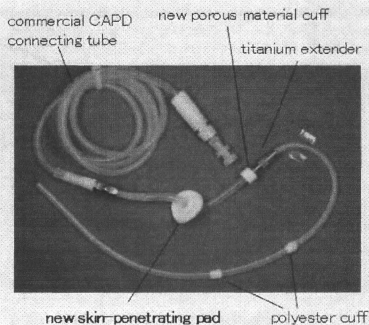
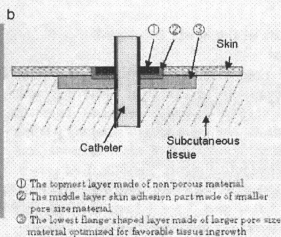


FIG. 5. Photograph of the skin-penetrating pad and porous material cuff connected to a CAPD catheter by using a titanium extender.

by absorbing the external pressure to the catheter (Fig. 4). Thanks to this structure, this device was thought to very firmly adhere to the skin, highly preventing infection. In order to study the biocompatibility of this pad and its effects on exit-site infection, we created prototypes of the skin-penetrating pad and surgically implanted them on the back skin of an adult goat that was kept under observation over a 2-year period. No wound care such as disinfection and draping was conducted except for the acute phase immediately after surgery. In addition, the skin-penetrating pad and porous material cuff were connected to a commercial CAPD catheter by using a titanium extender (Fig. 5), which was surgically placed long term into the abdominal cavity and subcutaneously tunneled and exteriorized. The goat



- ① The topmost layer made of non-porous material
- ② The middle layer skin adhesion part made of smaller pore size material
- ③ The lowest flange shaped layer made of larger pore size material optimized for favorable tissue ingrowth

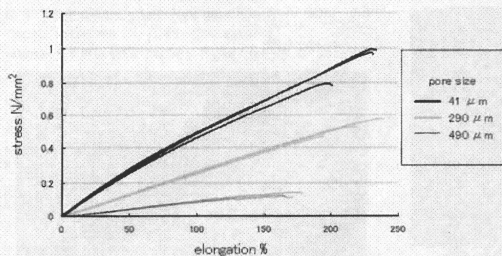


FIG. 6. Stress-strain curves of our porous materials.

actually underwent peritoneal dialysis (once a week, 2000 mL peritoneal dialysate) and was kept under observation for 120 days. After both experiments, the catheter was extracted, and pathological analysis was carried out. As the control, a polyester cuff was used, and the difference with our porous material was also studied. These experiments were conducted based on the Animal Experiment Guidelines of the National Cardiovascular Center under the approval of its Animal Experiment Committee.

RESULTS

Development of a new, segmented polyurethane porous material

The results of the tensile test showed that, upon rupture, the test material with an average pore diameter of 490 μm had a mean stress of 0.13 N/mm^2 and a mean elongation rate of 167% (86.93%); that, with an average pore diameter of 290 μm , had a mean stress of 0.52 N/mm^2 and mean elongation rate of 215% (822.03%); and that, with an average pore diameter of 41 μm , had a mean stress of 0.92 N/mm^2 and mean elongation rate of 219% (819.05%) (Fig. 6).

Biocompatibility of the newly developed porous material

Histological examination of the test tubes implanted to evaluate the extent of tissue ingrowth after 1 month showed granulation tissue ingrowth from both ends of the cylindrically shaped porous material, making separation of the material and living tissue extremely difficult. The length of granulation tissue ingrowth in the test tube was 4.0 ± 0.7 , 5.4 ± 0.9 , 6.6 ± 0.6 , and 7.2 ± 1.2 cm for the test materials with average pore diameters of 50, 150, 300, and 500 μm , respectively ($n = 5$), and, for the materials with pore diameters of 50–300 μm , the larger

the pore size, the greater was the extent of tissue ingrowth. For the materials with pore diameters of 300 μm and more, the length of tissue ingrowth formed a plateau at approximately 7.0 cm (Fig. 7). Histopathologically, the materials with large pore diameters (300–500 μm) had favorable mature adhesive tissue ingrowth mainly consisting of collagenous fibrous tissue, and tissue vascularization at the same site was also frequently observed. In addition, there was no infection or necrosis of the ingrown tissue in all of the groups.

Development of a CAPD catheter skin-penetrating pad and cuff using the newly developed porous material

Throughout the 2-year experimental period, there was no indication of infection such as reddening, swelling, or purulent discharge of the skin around the device or any spontaneous desquamation as a reaction to rejection of foreign material, and the pads tightly adhered to the skin. Every day, the catheter

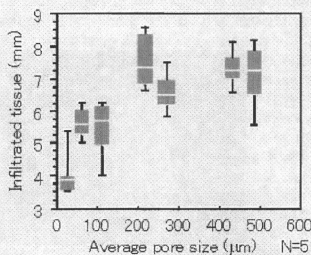


FIG. 7. The extent of tissue ingrowth increased in proportion to material pore size.

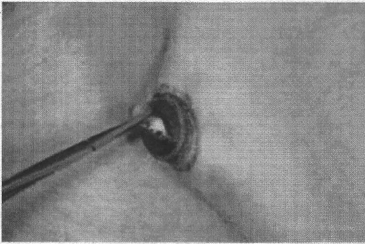


FIG. 8. Photograph of the implanted skin-penetrating pad. There was no infection or rejection of foreign material, and the pads tightly adhered to the skin. There was also no damage to the pad itself.

part was strongly pulled in various directions, but there was no subcutaneous disturbance of the flange part or damage to the pad itself (Fig. 8). When the extracted specimen was observed from the side of the subcutaneous tissue, the flange part was abundantly covered with vascularized tissue. There were no other findings such as abscesses under the skin. When the specimen was sliced along the catheter, no pocket formation due to epidermal downgrowth at the outer edge of the topmost layer was seen. The lowest layer was integrated with the surrounding tissue by abundant tissue ingrowth and could not be separated (Fig. 9). In the dialysis experiment using the CAPD catheter equipped with the skin-penetrating pad and cuff, the dialysate could be infused and drained without problem, and there was no damage such as detachment of the device from the skin despite considerable external pressure load to the catheter during infusion and drainage. Histological analysis showed that the ingrown granulation tissue between the fibers of the polyester cuff was mainly immature

granulation tissue mostly consisting of fibroblastic cells, but the ingrown granulation tissue in the porous material cuff was mainly mature collagenous fibrous tissue (Fig. 10).

DISCUSSION

As our basic approach toward the development of the new skin-penetrating pad, the following three points were taken into consideration: (i) selecting a polymeric material that has favorable biocompatibility and superior long-term mechanical and chemical durability; (ii) developing a material that has a continuous porous microstructure that can tightly adhere to the subcutaneous tissue; and (iii) designing a macrostructure that can disperse the repeated external pressure from the catheter and prevent epidermal downgrowth.

We selected Miracran, which is a polycarbonate segmented polyurethane resin, as the polymeric material. This material is used in undulating artificial heart diaphragms and has superior mechanical durability and flexibility. As it is also hypoallergenic, we decided that it was appropriate to use as the material for our skin-penetrating pad. From this, we succeeded in producing a new porous material that fitted our purposes using a newly developed manufacturing process (patent pending), enabling the pore diameter and pore rate to be adjusted. As for the macrostructure, we devised a three-layer structure, with each layer consisting of the material featuring different characteristics, efficiently dispersing the external pressure from the catheter and preventing epidermal downgrowth.

The newly developed porous material firmly adhered to the surrounding tissue when implanted and maintained flexibility with little burden on the surrounding tissue as well as having enough strength against external force, even though it had a pore size

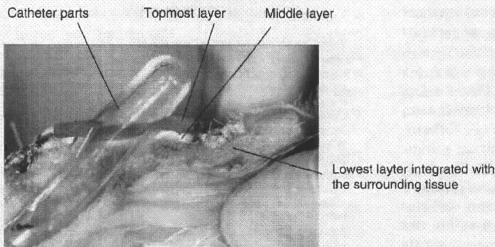


FIG. 9. Photograph of the specimen sliced along the catheter. No pocket formation due to epidermal downgrowth at the outer edge of the topmost layer was seen. The lowest layer was integrated with the surrounding tissue by abundant tissue ingrowth and could not be separated.

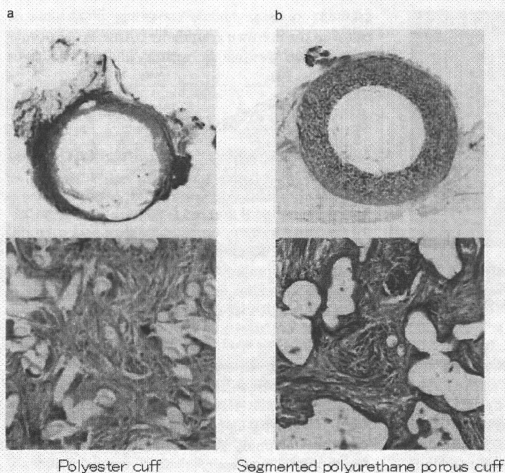


FIG. 10. Histological analysis showed that the ingrown granulation tissue between the fibers of the polyester cuff was mainly immature granulation tissue mostly consisting of fibroblastic cells (a), but the ingrown granulation tissue in the porous material cuff was mainly mature collagenous fibrous tissue (b).

that enabled sufficient ingrowth of granulation tissue and vascularization. The granulation tissue that infiltrated the porous material was mature and abundant in collagenous fibers compared with the polyester nonwoven material, which also indicated that it was effective in maintaining long-term adhesion. Furthermore, the novel skin-penetrating pad did not require any wound care including disinfection during the 2-year experimental period, and there was no indication of exit-site infection such as necrosis of the surrounding tissue or other infection during the experiment as well as at autopsy, demonstrating that it was effective for the inhibition of epidermal downgrowth.

The predicted advantages of the clinical application of this novel skin-penetrating pad are as follows: (i) the improvement of patient quality of life because the patient is liberated from exit-site care; (ii) decrease in the amount of disinfectants, film dressing materials, and antibiotics needed for catheter care; and (iii) decrease in treatment frequency of catheter problems such as exit-site infection with an accompanying reduction in medical cost. As a disadvantage, the skin and subcutaneous tissue must be removed when the skin-penetrating pad is removed with the catheter, but this is believed to be well within the range of tolerance, considering its major merits

such as simplified management and suppression of infections.

CONCLUSION

The newly developed segmented polyurethane porous material had excellent strength, flexibility, durability, biocompatibility, and tissue ingrowth. The novel skin-penetrating pad, which was devised by using this material, firmly adhered to the tissue and did not cause epidermal downgrowth at the site of catheter penetration, which suggested that it may be effective in preventing exit-site infection.

REFERENCES

1. Twardowski ZJ. Peritoneal access: the past, present, and the future. *Contrib Nephrol* 2006;150:195-201.
2. Knabe C, Grosse-Siestrup C, Gross U. Histologic evaluation of a natural permanent percutaneous structure and clinical percutaneous devices. *Biomaterials* 1999;20:503-10.
3. Gokeo CF, Lelah MD, Hauck W, Burhop KE. External catheter immobilization improves wound healing in micropigs. *ASAIO Trans* 1989;35:412-4.
4. Thodis E, Bhaskaran S, Psadakis P, Bargman JM, Vas SI, Oreopoulos DG. Decrease in staphylococcus aureus exit-site infections and peritonitis in CAPD patients by local application of mupirocin ointment at the catheter exit site. *Perit Dial Int* 1998;18:261-70.
5. Annigeri R, Conly J, Vas S, et al. Emergence of mupirocin-resistant staphylococcus aureus in chronic peritoneal dialysis

- patients using mupirocin prophylaxis to prevent exit-site infection. *Perit Dial Int* 2001;21:554-9.
6. Amano I, Katoh T, Inagaki Y. Development of alumina ceramic transcatheter connector to prevent skin exit site infections around CAPD catheters. *ASAIO Trans* 1990;36:M494-6.
 7. Paquay YC, de Ruijter JE, van der Waerden JP, Jansen JA. Tissue reaction to Dacron velour and titanium fibre mesh used for anchorage of percutaneous devices. *Biomaterials* 1996; 17:1251-6.
 8. Bay WH, Vaccaro PS, Powell SL, Erlich LF. The Gore-Tex peritoneal catheter: a clinical evaluation and comparison with the Tenckhoff catheter. *Am J Kidney Dis* 1984;4:268-79.
 9. Daly BD, Dasse KA, Gould KE, et al. A new percutaneous access device for peritoneal dialysis. *ASAIO Trans* 1987;33: 664-71.

Forward Osmosis Process for Dialysis Fluid Regeneration

Khaled Mohamed Talaat

Department of Internal Medicine, Faculty of Medicine, Zagazig University, Zagazig, Egypt

Abstract: In a preliminary experiment, 38% of the spent dialysis fluid water was reclaimed by a forward osmosis process through a cellulose triacetate membrane. The simplicity of forward osmosis and its minimal external energy requirements may allow the construction of a small bulk device that can reclaim a considerable portion of the water used in the patient's dialysis process. For developing an acceptable ambulatory dialysis system, decreasing the bulk of the fluid and equipment carried on the patient is essential. Forward osmosis may feasibly be used for dialysis fluid regeneration in ambulatory dialysis systems. **Key Words:** Ambulatory—Dialysis—Dialysis solution regeneration—Osmosis—Forward osmosis.

In the forward osmosis process, water is drawn across a water-permeable but solute-impermeable membrane from the feed solution into the more concentrated draw solution down the concentration gradient (1). The cellulose triacetate (CTA) membrane was made by Hydration Technologies, Inc. (Albany, OR, USA). The CTA membrane has outperformed other membranes in forward osmosis applications. The structure and the performance of this membrane have been reviewed (2-3). An example of the current applications of forward osmosis is the hydration bags made by Hydration Technologies, Inc. Hydration bags consist of an external feed solution compartment that is filled with either sea water or unsafe water, and an internal draw

solution compartment made of the CTA membrane. Water is drawn from the feed solution through the CTA membrane to dilute a concentrated sugary draw solution generating a safe-to-drink sugary beverage. In the current investigation, the potential use of the forward osmosis process for dialysis fluid regeneration was examined. A concentrated sodium chloride solution was used to draw water from the spent dialysis fluid across the same CTA membrane.

MATERIALS AND METHODS

In the current investigation, a sample of the spent dialysis fluid was collected 15 min after starting the patient's dialysis session. Before starting the forward osmosis experiment, the CTA membrane of the osmosis bag (the SeaPack made by Hydration Technologies, Inc.) was prehydrated by washing the two compartments of the osmosis bag with 0.45% saline. The saline was then drained before introducing 250 mL of the spent dialysis fluid into the feed solution compartment and 20 mL of 10% sodium chloride (Na^+ concentration = 1711 mmol/L) into the draw solution compartment. The forward osmosis process was carried out for 3 h at 35°C, while the osmosis bag was shaken on an automatic shaker that delivered 10-cm horizontal displacement at a frequency of 60 cycles/min. These experimental settings were found to increase the water reclamation rate in the initial trials. The feed and the draw solution were drained hourly. Their volume and sodium concentration were then determined before reintroducing them into the forward osmosis bag. Creatinine, urea, uric acid, phosphate, sodium, potassium, calcium, and magnesium were measured in the feed solution at the start of both experiments and in the draw solution at the end of the experiment. Water reclamation ratio was calculated as the gain in the draw solution volume / 250 × 100%. Sodium back-leak into the feed solution was calculated as the decrease in the Na^+ content of the draw solution / its initial Na^+ content at the start of the experiment × 100%. In the initial stages of the experiment, a search for the best settings that gave the highest water reclamation rate was done. The previously described shaking, membrane prehydration, and temperature gave the optimal results. The best obtained results were represented.

RESULTS

At the start of the experiment, the concentration of urea in the spent dialysis fluid solution was 32 mmol/L, creatinine 796 μmol/L, uric acid 635 μmol/L, calcium 1.1 mmol/L, magnesium

doi:10.1111/j.1525-1594.2009.00816.x

Received June 2008; revised October 2008.

Address correspondence and reprint requests to Professor Khaled Mohamed Talaat, Department of Internal Medicine, Faculty of Medicine, Zagazig University, Zagazig, PO 44519, Egypt. E-mail: k_m_talaat@yahoo.com

Artif Organs, Vol. 33, No. 12, 2009

Initial in vivo evaluation of the newly developed axial flow turbo pump with hydrodynamic bearings

Hideyuki Tanaka · Tomonori Tsukiya · Eisuke Tatsumi · Toshihide Mizuno · Tatsuya Hidaka · Takeshi Okubo · Toshiyuki Osada · Shinji Miyamoto · Yoshiyuki Taenaka

Received: 4 June 2009 / Accepted: 25 November 2010 / Published online: 5 January 2011
© The Japanese Society for Artificial Organs 2010

Abstract An implantable, compact rotary blood pump has been newly developed using an axial flow turbo pump with hydrodynamic bearings. The rotating impeller, which is hydrodynamically levitated with the assistance of repulsive magnetic force, has no contact with the inner surface of the pump. To evaluate the hemodynamic performance and biocompatibility, the pump was installed into four calves for up to 90 days. The pump was installed in the left heart bypass fashion, and placed paracorporeally in the first two calves and in the thoracic cavity in the other two calves. All calves received anticoagulation and anti-aggregation therapy during the study. Aortic pressure, heart rate and pump-operating parameters were continuously measured. Hematologic and biochemical tests to evaluate anemia, hepato-renal function and the extent of hemolysis were performed on schedule. Each calf was killed at the termination of the experiments, and pathological analysis for the biocompatibility of the pump system was performed, including the thrombi in the device, emboli in the systemic organs and signs of infection. The pump stably produced a flow of 5 l/min. Each calf was supported for 78, 50, 90 and 90 days, respectively, with no incidence of

hemorrhage, organ failure or significant hemolysis. No thrombus formation or mechanical wearing was observed inside the pump. There was no evidence of heat injury around the pump. Device-related infections were observed, but the severity of infection was mild in the implant case compared to the paracorporeal case. The pump demonstrated acceptable hemodynamic performance and biocompatibility in the initial in vivo testing.

Keywords Axial flow turbo pump · Hydrodynamic bearing · Left ventricular assist device

Introduction

Heart failure is a major health problem, and it affects more than 23 million people in developed countries [1]. Optimal drug therapy has been shown to benefit patients with heart failure, but the prognosis of end-stage heart failure and the quality of life of the patients remain extremely poor. Heart transplantation is the only curative treatment for end-stage heart failure; however, it has become a treatment option available to few because of the shortage of donor hearts. To resolve this problem, works on mechanical circulatory support, especially a left ventricular assist device (LVAD), have been promoted since the early 1960s; currently, implantable LVADs have become invaluable not only for bridging the time to transplantation, but also for myocardial recovery and destination therapy as permanent support for patients ineligible for transplantation [2–4].

The efficacy of long-term LVAD support for patients with advanced heart failure was demonstrated by the results of a randomized clinical trial that evaluated the clinical outcome of treatment with a pulsatile flow device [4]. This trial compared the clinical outcome of treatment with a pulsatile flow

H. Tanaka · T. Tsukiya (✉) · E. Tatsumi · T. Mizuno · Y. Taenaka
Department of Artificial Organs, The Advanced Medical Engineering Center, Research Institute, National Cardiovascular Center, 5-7-1 Fujishiro-dai, Suita, Osaka 565-8565, Japan
e-mail: tsukiya@ri.nccv.go.jp

T. Hidaka · T. Okubo · T. Osada
Mitsubishi Heavy Industries, Ltd., Takasago, Hyogo, Japan

H. Tanaka (✉) · S. Miyamoto
Department of Cardiovascular Surgery, Faculty of Medicine, Oita University, Hasama-nachi, Yufu, Oita 879-5593, Japan
e-mail: tanakah@med.oita-u.ac.jp

device with that with optimal medical management, and reported that treatment with a LVAD significantly improved the possibility of survival at 2 years [4]. However, this trial revealed some limitations of a pulsatile flow device: the large size of the pump, limited device durability and clinical adverse effects such as thromboembolic events [4]. Development of the LVAD systems using continuous flow blood pumps have overcome some of these problems with their compact structure. The blood flow in the continuous flow pumps is usually thoroughly studied in the design stage to eliminate the stagnant area in the device and to minimize the mechanical damage of the blood cell components. Consequently, several devices are currently available that allow patients to leave the hospital with an enhanced quality of life. The results of a randomized clinical trial comparing the clinical outcome of treatment with a pulsatile flow device with that of a continuous flow device have been reported [5]. Superior actuarial survivals free of stroke and device failure at 2 years were revealed in patients with a continuous flow LVAD in comparison with a pulsatile flow LVAD [5]. However, continuous flow blood pumps that contain a mechanical contact bearing have limitations in durability and the potential risk of thrombus formation because of mechanical wear and heat generation originating from the mechanical contact points. To overcome these problems, some innovative technologies, such as a magnetic or hydrodynamic levitation system, have been applied to the new generation of rotary blood pumps. These pumps, supporting the rotating impeller without using seals or mechanical contact, can work without any material wear, reducing the risk of thrombogenic complications. These pumps are conceived to increase the feasibility of reliable circulatory support.

Our research group is collaborating with Mitsubishi Heavy Industry Ltd. (Takasago, Hyogo, Japan) on the development of a small, implantable axial flow pump in which the rotating impeller is fully levitated with the hydrodynamic bearings. In the present study, we carried out chronic animal experiments using calves in the fashion of a left ventricular bypass to evaluate the hydrodynamic performance and biocompatibility. The objective of this study was to evaluate the biocompatibility of the pump, including the antithrombogenicity of the pump with a standard anticoagulation therapy, the hemolytic properties caused by the pump, the damage of the surrounding tissues by the implantation of the pump and the hydrodynamic properties as a LVAD.

Materials and methods

Animal model

Four healthy Holstein calves that weighed between 80 and 98.7 kg were used in this study. The axial flow pump was

installed in the fashion of a left ventricular bypass to the descending aorta. The pump was paracorporeally installed in the first two animals (case 1 and 2), whereas it was implanted into the thoracic cavity in the other two (case 3 and 4). All calves received humane care during the entire experimental periods. These experiments were conducted based on the Animal Experiment Guidelines of the National Cardiovascular Center under the approval of its Animal Experiment Committee.

The device

The blood pump used in this study is an axial flow pump that has been developed as an implantable LVAD. The axial flow pump has the dimensions of 29 mm in diameter and 75 mm in length. The weight of the pump is 150 g, and the displaced volume is approximately 50 ml. The priming volume of the pump is 10 ml. A photograph and schematic cross section of the axial flow pump are shown in Fig. 1. The impeller, which is the single moving part of the pump, is placed in the space between the stationary casing, the inlet guide part and the diffuser. The central shaft connects the inlet guide part and the diffuser through the bore of the impeller. The impeller rotates around the shaft with a narrow clearance smaller than 100 μ m. The blood film in this clearance works as the journal bearing, which generates sufficient pressure to sustain the mechanical load on the impeller to avoid mechanical contact with the stationary parts. The axial thrust, on the other hand, is passively balanced with the help of the repulsive force generated by the permanent magnets embedded in the impeller body and the inlet guide part. As a result of these passively supported bearings, no position sensors are needed. In glycerin solution with a viscosity of 3 mPa S, a pump flow of 5 l/min against the pump head of 100 mmHg was achieved at 9,000 rpm. The hemolytic properties of this pump were considered to be within the acceptable range for clinical use, as reported in the previous study [6].

The outflow graft used in this study was attached to the flexible outflow cannula, made of polyvinyl chloride, with an inner diameter of 12 mm. The outflow graft was connected to the blood pump through the outflow cannula. Two types of inflow cannula, flexible and rigid cannula with an inner diameter of 12 mm, were prepared, and each cannula was separately used according to the difference of pump placement. A flexible cannula made of polyvinyl chloride was used for paracorporeal placement; in contrast, a rigid cannula made of titanium alloy, which was attached to the pump, was used for intrathoracic placement. An apical cuff with a sewing ring was used to secure the inflow cannulas to the myocardium.

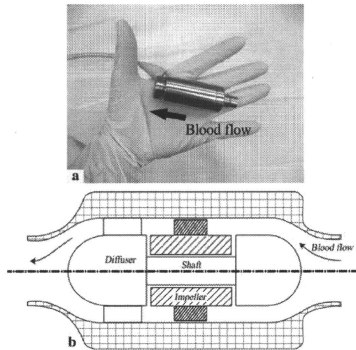


Fig. 1 a Newly developed axial flow turbo pump with a flexible power cable. The external dimensions of the pump are 29 mm in diameter and 75 mm in length. The weight is approximately 150 g, and the volume replacement is approximately 50 ml. The priming volume of the pump is approximately 10 ml. **b** Cross section of the pump

Surgical preparation

Animals were sedated by intramuscular injection of ketamin hydrochloride (5–10 mg/kg). Each animal was placed in a right lateral recumbent position and instrumented with an electrocardiogram to monitor the heart rate. A 16-F double-lumen venous catheter was inserted into the left external jugular vein to administer agents. Each animal was intubated with an orotracheal tube and mechanically ventilated. General anesthesia was then introduced and maintained with isofurane (0.5–3%) in oxygen (50–70%).

Surgical procedures

Left fifth subcostal thoracotomy was performed. An 18-F single-lumen catheter was inserted into the left mammary artery to monitor the aortic pressure. Surgery was performed without a cardiopulmonary bypass. After the descending aorta was exposed, the outflow graft was anastomosed there in an end-to-side fashion. An apical cuff with a sewing ring was fixed around the left ventricular apex. After heparinization, the left ventricular apex was cored with a circular knife, and the inflow cannula was inserted into the left ventricular cavity and secured. In case 1 and 2, the outflow cannula was exteriorized through the thoracotomy wound, and the inflow cannula was passed through the chest wall and tunneled to exteriorize near the

left lateral abdominal area. The driveline was directly connected to the external controller. The pump was started with low pump speed and placed around the left lateral abdominal area. In case 3 and 4, the driveline was tunneled to exteriorize near the left paraspinous area. The pump was started and placed around the cost-phrenic portion to avoid compression of the lung. The pump speed was gradually increased up to approximately 9,000 rpm and then manually controlled to have flow rates of 5–6 l/min. A blood flow probe (MFV-2100, Nihonkouden, Japan) to measure the pump flow was attached to the outflow graft, and a thermocouple temperature probe (RET-1, Physitemp Instruments, Inc., USA) was placed on the pump surface. Two chest tubes were inserted into the thoracic cavity. After intercostal nerve block, the chest cavity was closed in the usual fashion.

Postoperative care

The calves were transferred to a cage in the experimental room for continuous monitoring of heart rate, aortic pressure, pump flow and pump surface temperature. They were allowed to eat for several hours after extubation. Each calf received oral administration of warfarin potassium (Warfarin[®], Eisai Co., Ltd., Tokyo, Japan) and aspirin (Bayaspirin[®], Bayer Yakuhin Co., Ltd, Osaka, Japan), and the PT-INR (DRIHEAMAT CGO2V, Atwill, Japan) was controlled at a range of 2.0–3.0 times the preoperative value. Daily observation of the feed intake, urine volume, respiratory rate, neurological status and wounds was performed for evaluating the general status of the calves.

Data collection

In all calves, aortic pressure and heart rate were continuously measured during the experimental periods. As pump-operating parameters, pump flow, pump speed and power consumption were also continuously measured. To evaluate end-organ function, extent of hemolysis and anemia, blood samples were obtained at 1, 3 and 7 postoperative days, and thereafter once a week until termination of the experiment. Blood cell counts and biochemical tests (Vet Scan[®], Abaxis, Inc., USA) were performed to measure hemoglobin, serum creatinine, blood urea nitrogen (BUN), aspartate aminotransferase (AST) and the total bilirubin level in each sample. The extent of hemolysis was qualitatively assessed by the chemistry analyzer; the chemistry analyzer can detect hemolysis and assess its degree in four qualitative levels from 0 to (3+), based on the free hemoglobin level in a blood sample. Qualitative negative is equivalent to less than 20 mg/dl as free hemoglobin level, (1+) to 20–40, (2+) to 40–60 and (3+) to more than 60 mg/dl, respectively. In addition, pump surface

Table 1 Pump setting, duration of support, mean pump flow, mean pump speed, mean aortic pressure, pump temperature and cause of termination in four calves supported by the newly developed axial pump

Case	Body weight (kg)	Setting	Duration (day)	Mean flow (mmHg)	Speed (rpm)	AoP (mmHg)	Temperature (°C)	Termination
1	89.4	Paracorporeal	78	6.2 ± 0.9	9,085 ± 269	100 ± 7.8	–	Decreasing in flow
2	88	Paracorporeal	50	5.2 ± 1.3	9,765 ± 526	111 ± 8.0	–	Decreasing in flow
3	98.7	Intrathoracic	90	4.7 ± 0.5	8,989 ± 114	101 ± 5.5	40.2 ± 0.7	Schedule
4	80	Intrathoracic	90	5.4 ± 0.6	8,520 ± 264	90 ± 12	39.8 ± 0.5	Schedule

Data are the mean ± SD

AoP aortic pressure

temperature was also continuously measured in case 3 and 4. At the termination of each experiment, pathological analysis for the biocompatibility of the pump system was performed, including the thrombi in the device, emboli in the systemic organs and signs of infection. The animals were killed after administration of heparin to prevent clotting in the prostheses, and then the device was uninstalled. All removed specimens were rinsed gently with saline solution to remove excess intraluminal blood and inspected grossly and histologically. In case 3 and 4, the presence of heat injury and waterproofing of the pump were also examined.

Results

Each calf was supported for 78, 50, 90 and 90 days, respectively. In case 1 and 2, experiments were terminated because of the irreversible decrease in the pump flow caused by graft kinking and an inflow cannula obstruction associated with a wedge thrombus and cellular fibrous tissue growths at the LV apex, respectively. In contrast, scheduled terminations were achieved in case 3 and 4. None of the four calves developed anorexia, respiratory or neurological disorders.

Pump performance

A summary of the pump operating parameters and hemodynamic measurements is shown in Table 1. The pump stably produced a mean flow rate of 5 l/min, and the variation of the mean flow rates was in the range of the mean flow rate ± 1 l/min without major variation of the rotational speed. The power consumption was within the range of 6–6.5 W in all cases. The hemodynamics were stable throughout the entire period excluding the acute phase after surgery in all cases. The records of the waveform of the pump flow and aortic pressure in case 3 are shown in Fig. 2. These waveforms were recorded while the rotational speed was temporarily varied from 6,000 to 10,000 rpm in order to investigate the maximum flow rate. The pump flow

increased in proportion to an increase in the pump speed, achieving up to 8 l/min at the peak and over 5 l/min in mean value at 10,000 rpm. The waveform of aortic pressure showed a reduction of the amplitude with increasing pump flow, demonstrating that the pump progressively unloaded the left ventricle with continuous flow. Figure 3 shows the trends of the mean heart rate, mean aortic pressure and mean pump surface temperature as recorded in case 3. Tachycardia in the range of 120–140 beats per minute was observed after surgery, and then it gradually improved without intervention. The heat generation, while the pump was operating, was within the tolerable range. The maximum surface temperature of the pump was 41°C.

Biological data

The biochemical and hematological data are shown in Fig. 4. The hemoglobin level was stable during the experimental periods, excluding a transient decrease that occurred after surgery. The serum creatinine, BUN, AST and total bilirubin levels were almost completely stable during the experimental periods. No marked alteration in these biochemical data was observed. Hemolysis was qualitatively shown to be negative throughout the experiments (Table 2).

Infection

In case 1 and 2, wound infections where the inflow cannula was exteriorized through the skin were observed. These conduit infections needed abscess drainage and daily wound irrigation until the termination of the experiment. In contrast, wound infection where the percutaneous driveline was exteriorized was observed in case 3; however, this driveline infection needed occasional wound irrigation. In case 4, there was no evidence of infection.

Necropsy findings

An examination of the device demonstrated that there were no depositions or thrombus formations inside the pump in